The following article appeared in Data in Brief Volume 21, December 2018, Pages 2350-2359; and may be found at: 10.1016/j.dib.2018.11.057

Data in Brief 21 (2018) 2350–2359

Contents lists available at ScienceDirect

Data in Brief

journal homepage: www.elsevier.com/locate/dib

Data Article

Experimental data in support of characterization of the $CePO_4$ dispersion into transparent PMMA/PU IPNs by the sequential route

D. Palma-Ramírez [a,*], M.A. Domínguez-Crespo [a,*], A.M. Torres-Huerta [a], V.A. Escobar-Barrios [b], H. Dorantes-Rosales [c], H. Willcock [d]

[a] *Instituto Politécnico Nacional, CICATA-Altamira, km 14.5 Carretera Tampico-Puerto Industrial Altamira, C.P. 89600 Altamira, Tamps., México*
[b] *IPICYT, División de Materiales Avanzados, SLP, México*
[c] *Instituto Politécnico Nacional, ESIQIE, Departamento de Metalurgia, C.P. 07300 Ciudad de México, México*
[d] *Department of Materials, Loughborough University, Loughborough LE11 3TU, United Kingdom*

ARTICLE INFO

Article history:
Received 1 June 2018
Accepted 12 November 2018
Available online 15 November 2018

ABSTRACT

This article is focused on the complementary data referring to the article "Dispersion of upconverting nanostructures of $CePO_4$ using rod and semi-spherical morphologies into transparent PMMA/PU IPNs by the sequential route". It contains the XPS data of $CePO_4$, photographs and DSC thermograms of transparent PMMA/PU IPNs as well as with $CePO_4$ dispersed in different wt.%, Confocal laser scanning micrographs, transmission electron microscopy (TEM), optical images of surface, and visual inspection (photographs) before and after aging of hybrid materials.

* Corresponding authors.
E-mail addresses: diana.palma@ujat.mx (D. Palma-Ramírez), mdominguezc@ipn.mx (M.A. Domínguez-Crespo).

https://doi.org/10.1016/j.dib.2018.11.057

Specifications table

Subject area	*Materials sciences*
More specific subject area	*Interpenetrating Polymer Networks (IPNs)*
Type of data	*Figures, Scheme and Micrographs, Images*
How data was acquired	*Differential scanning calorimetry (Labsys Evo,Setaram TGA/DSC), X-ray photoelectron spectroscopy, Confocal laser scanning microscopy (*Carl ZEISS LSM 700*), Transmission electron microscopy (JEOL* JEM-2000 FX*).*
Data format	*Raw data, plotted, analyzed.*
Experimental factors	*Samples were prepared as described in [1]. For TEM, samples were sputter coated with Au-Pd for 30 s on a Quorum Q150T ES sputter coater system.*
Experimental features	*$CePO_4$ powders and films of $CePO_4$/PMMA/PU IPNs, respectively, were analyzed.*
Data source location	*CICATA IPN Unidad Altamira, Tamaulipas, México.* *Materials Department, Loughborough University, United Kingdom.*
Data accessibility	*Data is with the article.*
Related research article	*D. Palma-Ramírez, M.A. Domínguez-Crespo, A.M. Torres-Huerta, V.A. Escobar-Barrios, H. Dorantes-Rosales, H. Willcock, Dispersion of upconverting nanostructures of $CePO_4$ using rod and semi-spherical morphologies into transparent PMMA/PU IPNs by the sequential route, Polymer 142 (2018) 356–374.*

Value of the data

- This data can be useful for comparing the dispersion of $CePO_4$ nanostructures in similar systems and how the morphology affects the structural, thermal and mechanical properties.
- Data highlights the influence of dispersed $CePO_4$ in different PMMA/PU ratios.
- This article will serve as a guideline to select the amounts adequate for dispersing $CePO_4$ into PMMA/PU.

1. Data

Plastic materials with good durability can be obtained from the synthesis of interpenetrating polymer networks (IPNs) while incorporating luminescent nanostructures such as Fluoro-functionalized nanostructured silica ($FSiO_2$), silica (SiO_2), carbon black (CB), barium titanate ($BaTiO_3$), polyaniline, and cerium phosphate ($CePO_4$) [1–6].

The dataset of this article shows additional information about the dispersion of $CePO_4$, in rods and semi-spherical morphologies, into transparent PMMA/PU IPNs. Initially, this study provides facts of the elements in $CePO_4$. For this reason, Fig. 1 shows the X-ray spectroscopy (XPS) spectra of nanorods and semi-spherical particles of $CePO_4$. This data also include photographs of different ratios of PMMA/PU that showed the transparency of the samples synthesized (Fig. 2). The thermal properties of PMMA/PU IPNs are confirmed in thermograms of selected PMMA/PU IPNs in Fig. 3. In addition, visual examination after incorporation of nanostructure in the polymer was analyzed. The incorporation, 0.1, 0.5, and 1 wt.% of $CePO_4$ (nanorods and semi-spherical) in 50/50 ratio of PMMA/PU IPNs is shown in photographs (Fig. 5). In this context, dispersion and emission properties of $CePO_4$/PMMA/PU IPNs is confirmed by confocal laser scanning images showed in Figs. 6 and 7. Dispersion of nanorods and semi-spherical $CePO_4$ was evaluated in a selected sample, 5O/50 PMMA/PU IPNs (Fig. 8). On the other hand, the texture of fractures from the tensile test is observed in Fig. 9. Finally, visual inspection before and after accelerated weathering test is seen in Fig. 10.

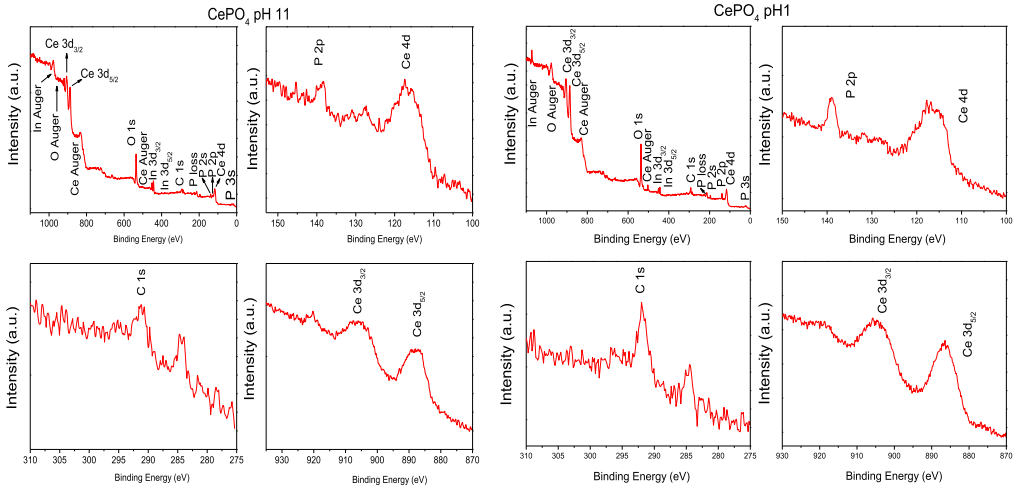

Fig. 1. XPS spectra of nanorods and semi-spherical $CePO_4$ nanoparticles.

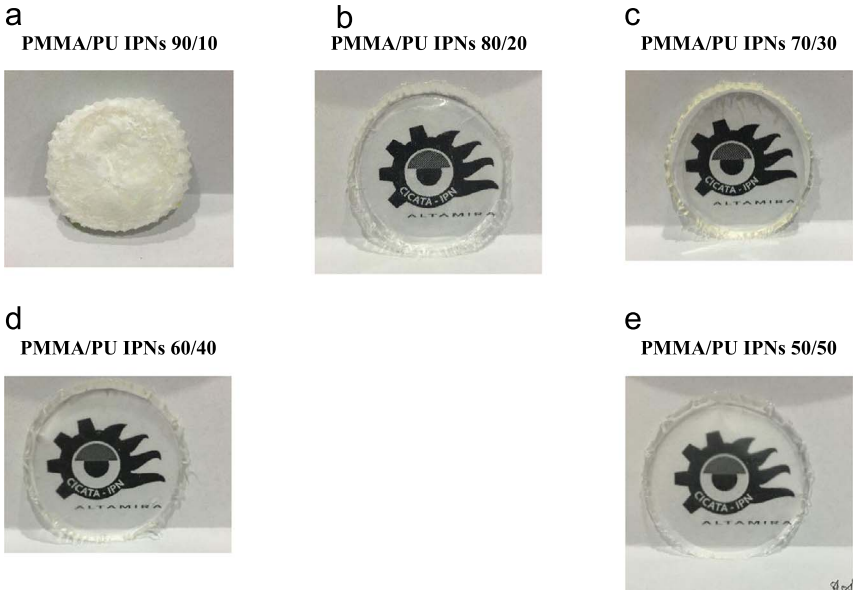

Fig. 2. Photographs of pure PMMA/PU IPNs in different ratios.

2. Experimental design, materials, and methods

2.1. Cerium phosphate ($CePO_4$) synthesis and characterization

$CePO_4$ nanostructures in nanorod and semi-spherical morphologies were obtained at pH 1 and 11, respectively, by the microwave-assisted hydrothermal method following the procedure described in Ref. [7].

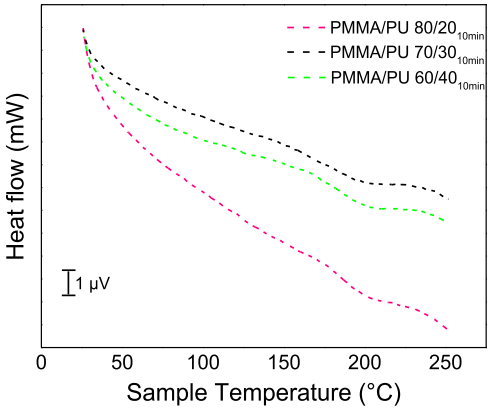

Fig. 3. DSC thermograms of PMMA/PU IPNs.

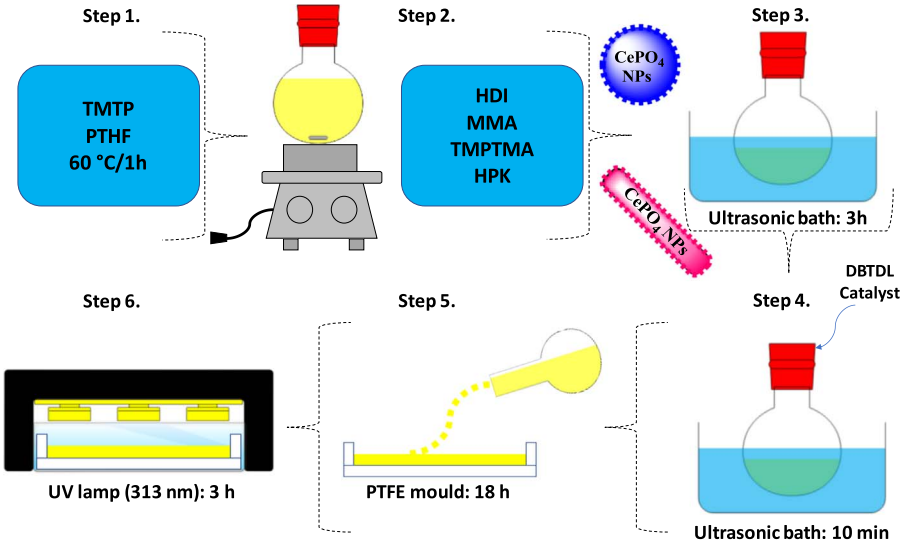

Fig. 4. Scheme of polymerization process of hybrid PMMA/PU/$CePO_4$ IPNs.

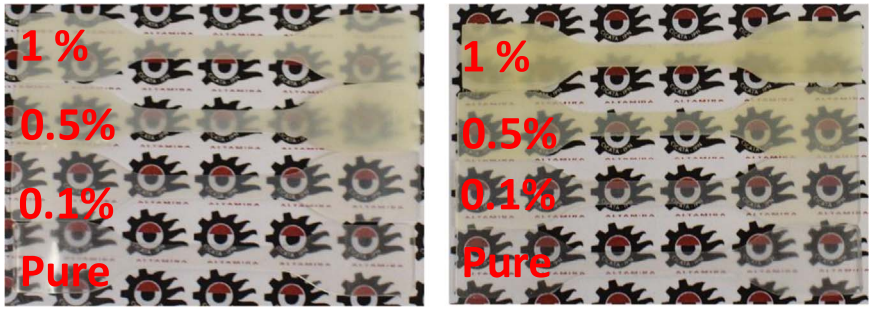

Fig. 5. Photographs of pure PMMA/PU IPNs (50/50 system) and PMMA/PU/$CePO_4$ IPNs (50/50 system) with the addition of nanorods (on the left) and semi-spherical (on the right) type morphologies.

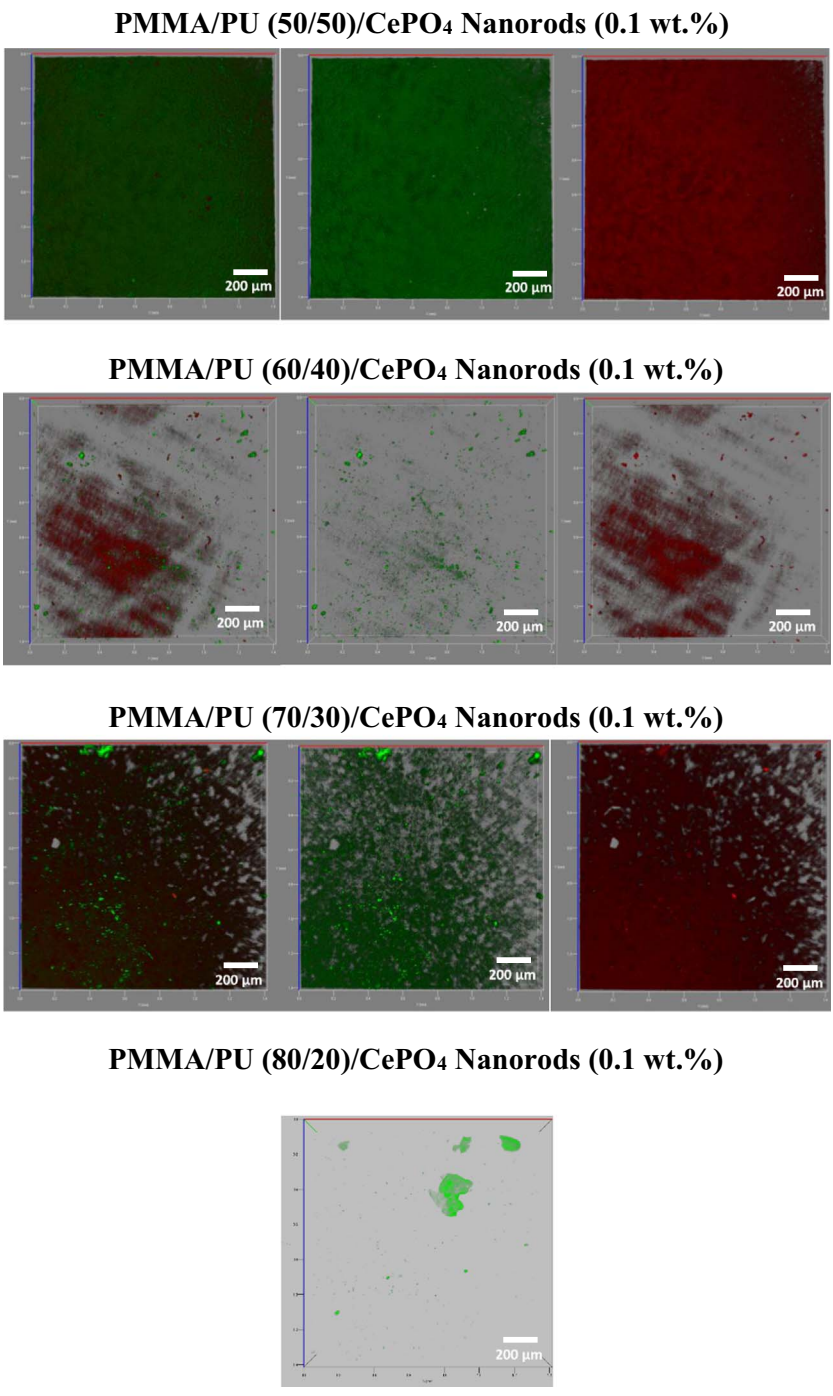

Fig. 6. CLSM images of $CePO_4$ nanorods in 0.1 wt.% into 50/50, 60/40, 70/30, and 80/20 ratio of PMMA/PU IPNs.

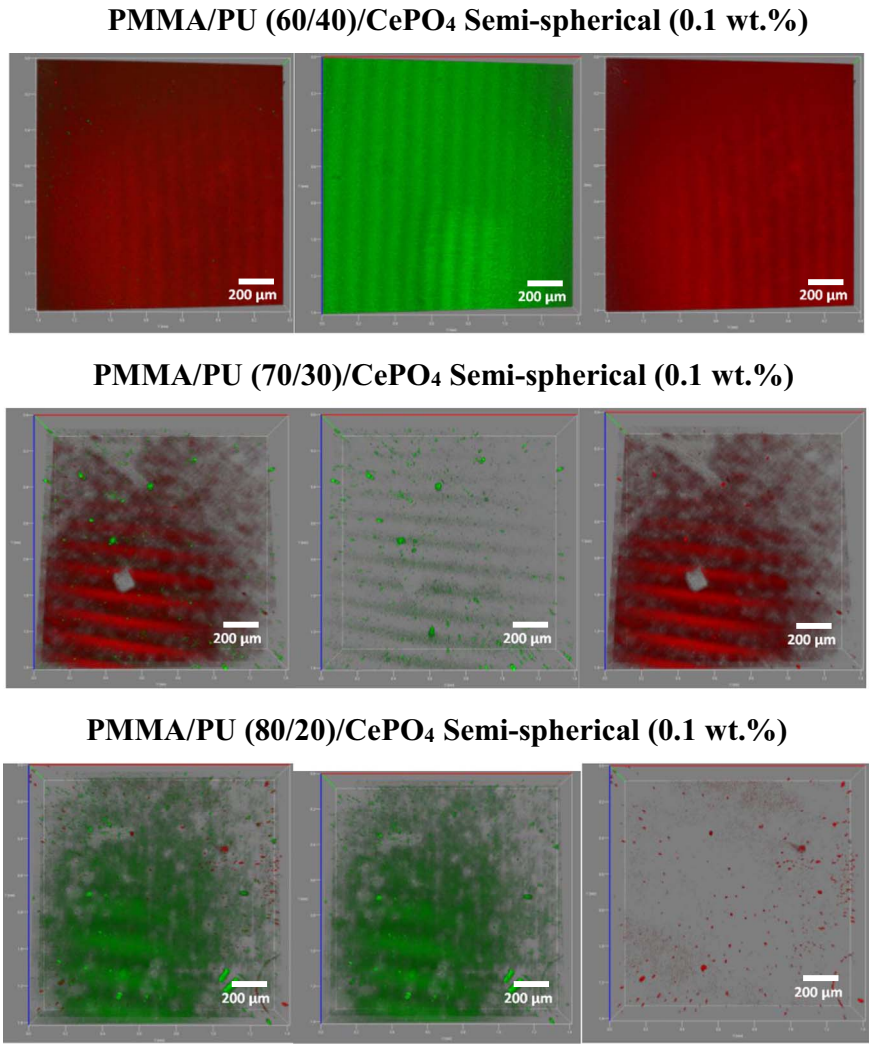

Fig. 7. CLSM images of $CePO_4$ semi-spherical in 0.1 wt.% into 60/40, 70/30, and 80/20 ratio of PMMA/PU IPNs.

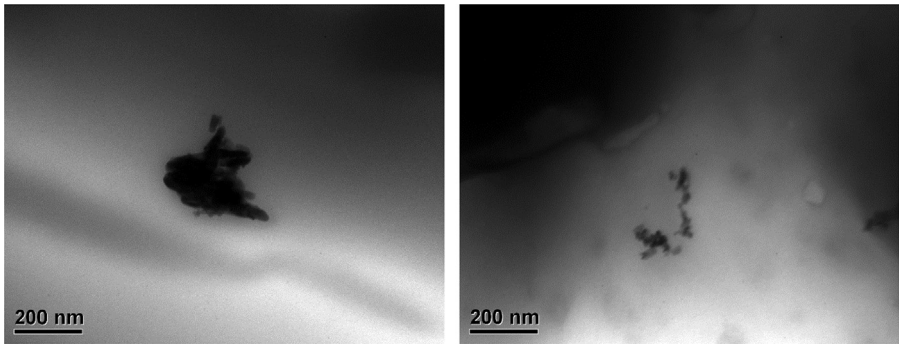

Fig. 8. TEM images of nanorods and semi-spherical $CePO_4$ nanoparticles dispersed in PMMA/PU 50/50 system.

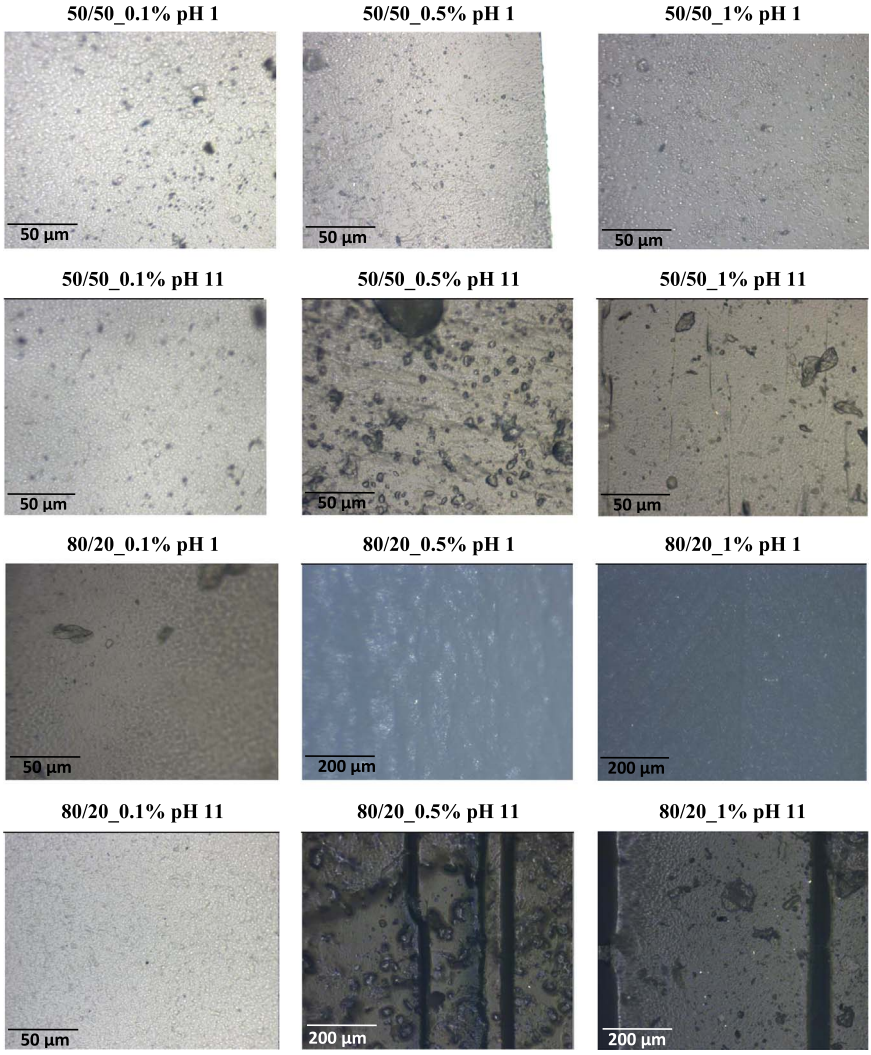

Fig. 9. Images of selected PMMA/PU/$CePO_4$ IPNs.

2.1.1. X-Ray photoelectron spectroscopy (XPS) test was assessed in an Alpha 110, ThermoFisher Scientific

XPS spectra of $CePO_4$ powders at two different pH are shown in Fig. 1. XPS spectra show typical binding energies of Ce^{3+} and Ce^{4+}, which are forming the chemical state of as-prepared powders. The results were used to confirm the chemical composition.

2.2. Sequential synthesis of PMMA/PU/IPNs and $CePO_4$/PMMA/PU/IPNs

IPNs were prepared following the procedure in Ref. [1]. The transparency of the different ratios of PMMA/PU was evaluated by visual examination of samples synthesized, as it is shown in Fig. 2.

Thermal properties of selected PMMA/PU pure samples were evaluated in Differential scanning calorimetry (DSC), conducted using a simultaneous Labsys Evo, Setaram TGA/DSC. Samples of DSC were tested at a heating rate of 10 K/min over the temperature range from 30 to 250 °C, under nitrogen atmosphere. Approximately 10–20 mg of each sample was placed in aluminium crucibles and maintained at 30 °C for 2 min, heated from 30 °C to 250 °C, maintained again at 250 °C for 2 min,

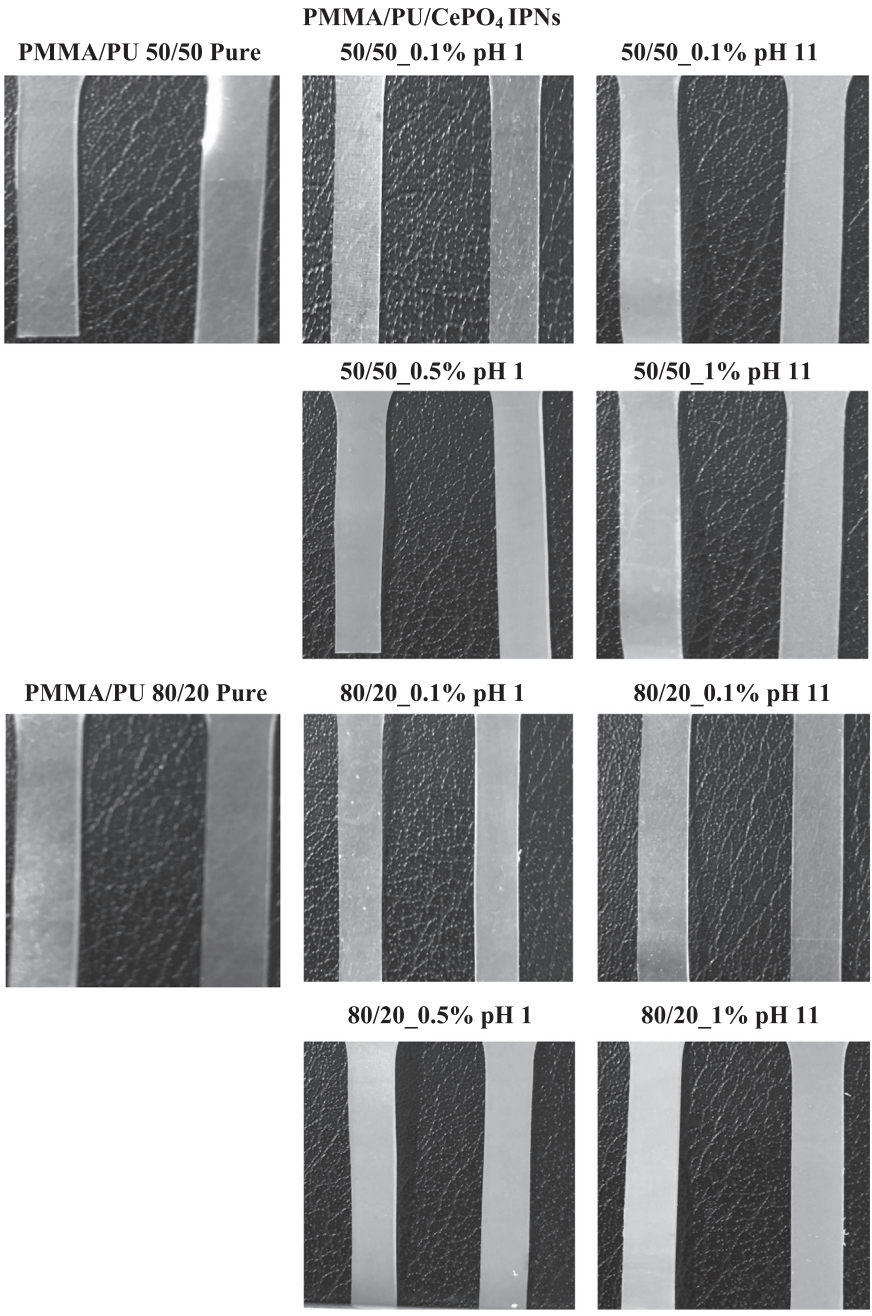

Fig. 10. Images of selected PMMA/PU/$CePO_4$ IPNs before (on the right) and after (on the left) aging during 500 h under heat and humidity conditions.

and cooled from 250 °C to 50 °C. PMMA/PU. Fig. 3 shows the thermograms corresponding to 60/40, 70/30, and 80/20 ratios of PMMA/PU.

Different amounts (0.1, 0.5, and 1.0 wt.%) of both nanostructures were incorporated and sonicated in the raw materials for PMMA and PU using two mixing times: 3 h and 10 min. DBTDL catalyst was added into the solution and sonicated for 10 min (Fig. 4). The final solution was poured into a PTFE mould and kept for 18 h and 3 h in UV lamp (363 nm).

Selected sample, PMMA/PU 50/50 ratio, is displayed in Fig. 5 showing the differences for each addition of nanorod and semi-spherical particles, respectively.

Dispersion of $CePO_4$ nanostructures in rod and semi-spherical morphologies within the PMMA/PU IPNs was performed by confocal laser scanning microscopy (CLSM) using a Carl ZEISS microscope (Carl Zeiss, Jena, Germany). The fluorescence intensity measurements were performed using the built-in software ZEN of the LSM 710. Results are shown in Figs. 6 and 7.

Transmission electron microscopy (TEM) was used to observe the dispersion of nanostructures in selected PMMA/PU/$CePO_4$ (50/50/1 wt.%). Ultra-thin sections were microtomed in epoxy resin. The sample was embedded and cured in R1078 Agar low viscosity resin (Agar scientific). The sample was shaped into a pyramidal shape and cut with a diamond knife into slices. A slice was put onto a Holey Carbon film 200 mesh Copper (HC200Cu). TEM observations were recorded in a JEM-2000 FX electron microscope (JEOL). Results are shown in Fig. 8.

The surface of PMMA/PU/$CePO_4$ IPNs in 80/20 and 50/50 ratio with 0.1, 0.5, and 1 wt.% of $CePO_4$ were analyzed in a were evaluated using an Olympus BX51 microscope. Results are shown in Fig. 9.

Selected dog-bone specimen of PMMA/PU/$CePO_4$ were subjected to aging under humid conditions using a climate chamber (Memmer GmbH equipment) at 55 °C and 85% relative humidity for 500 h. Photographs of physical changes are shown in Fig. 10.

Acknowledgments

D. Palma-Ramírez is grateful for her postgraduate fellowship to Consejo Nacional de Ciencia y Tecnología (CONACYT), México, Comisión de Operación y Fomento de Actividades Académicas del IPN (COFAA), México and Secretaría de Investigación y Posgrado (SIP) del Instituto Politécnico Nacional (IPN) México. Authors would like to thank to Loughborough Materials Characterisation Centre (LMCC), especially to Dr. Keith Yendall and Dr. Zhaoxia Zhou for their technical support and research assistance with this project. The authors are also grateful for the financial support provided by Instituto Politécnico Nacional through the SIP 2017-1186, 2018-0496 and 2018-1171, and COFAA; CONACYT through the CB-2015–252181 and SNI-CONACYT.

Transparency document. Supplementary material

Transparency document associated with this article can be found in the online version at https://doi.org/10.1016/j.dib.2018.11.057.

References

[1] D. Palma-Ramírez, M.A. Domínguez-Crespo, A.M. Torres-Huerta, V.A. Escobar-Barrios, H. Dorantes-Rosales, H. Willcock, Dispersion of upconverting nanostructures of $CePO_4$ using rod and semi-spherical morphologies into transparent PMMA/PU IPNs by the sequential route, Polymer *142* (2018) *356–374*.

[2] S. Fuina, G.C. Marano, G. Puglisi, D. De Tommasi, G. Scarascia-Mugnozza, Thermo-mechanical response of rigid plastic laminates for greenhouse covering, J. Agri. Eng. 47 (3) (2016) *7* (2016).

[3] W.S.Y. Wong, Z.H. Stachurski, D.R. Nisbet, A. Tricoli, Ultra-durable and transparent self-cleaning surfaces by large-scale self-assembly of hierarchical interpenetrated polymer networks, ACS Appl. Mater. Interfaces *8* (*21*) (2016) *13615–13623*.

[4] S.S. Ray, M. Bousmina, A. Maazouz, Morphology and properties of organoclay modified polycarbonate/poly(methyl methacrylate) blend, Polym. Eng. Sci. *46* (*8*) (2006) *1121–1129*.

[5] J.-M. Widmaier, G. Bonilla, in situ synthesis of optically transparent interpenetrating organic/inorganic networks, Polym. Adv. Technol. *17* (*9-10*) (2006) *634–640*.

[6] T. Phuttachart, N. Kreua-ongarjnukool, R. Yeetsorn, M. Phongaksorn, PMMA/PU/CB composite bipolar plate for direct methanol fuel cell, Energy Procedia *52* (2014) *516–524*.
[7] D. Palma-Ramírez, M.A. Domínguez-Crespo, A.M. Torres-Huerta, H. Dorantes-Rosales, E. Ramírez-Meneses, E. Rodríguez, Microwave-assisted hydrothermal synthesis of $CePO_4$ nanostructures: correlation between the structural and optical properties, J. Alloy. Comp. *643* (2015) (*S209-S218*.6/1/2018; 11/12/2018).